

Synthesis and Evaluation of Bifunctional [2.2.2]-Cryptands for Nuclear Medicine Applications

Anthony W. McDonagh, Brooke L. McNeil, Brian O. Patrick, and Caterina F. Ramogida*

Cite This: *Inorg. Chem.* 2021, 60, 10030–10037

Read Online

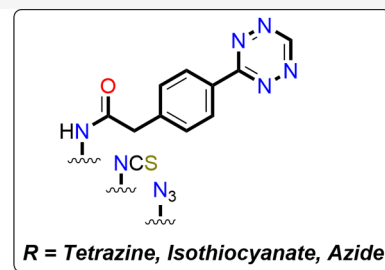
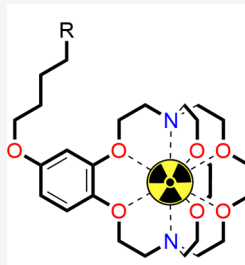
ACCESS |

Metrics & More

Article Recommendations

Supporting Information

ABSTRACT: For the first time, synthesis of bifunctional [2.2.2]-cryptands (CRYPT) and demonstration of radiolabeling with lead(II) (Pb^{2+}) isotopes are disclosed herein. The synthesis is convenient and high-yielding and gives access to three distinct bifunctional handles (azide ($-\text{N}_3$), isothiocyanate ($-\text{NCS}$), and tetrazine ($-\text{Tz}$)) that can enable the construction of radio-immunoconjugates for targeted and pretargeted therapy. Proof-of-principle CRYPT radiolabeling was successful with lead-203 (^{203}Pb) and demonstrated complexation efficiency superior to that of DOTA (1,4,7,10-tetraazacyclododecane-1,4,7,10-tetraacetic acid) and efficiency comparable to that of the current industry standard TCMC (1,4,7,10-tetraaza-1,4,7,10-tetra-(2-carbamoylmethyl)-cyclododecane). *In vitro* human serum stability assays demonstrated excellent ^{203}Pb -CRYPT stability over 72 h ($91.7 \pm 0.56\%$; $n = 3$). ^{203}Pb -CRYPT-radioimmunoconjugates were synthesized from the corresponding CRYPT-immunoconjugate or by conjugating ^{203}Pb -Tz-CRYPT to transcytlooctene modified trastuzumab (TCO-trastuzumab) via the inverse electron-demand Diels–Alder (IEEDA) reaction. This investigation reveals the potential for CRYPT ligands to become new industry standards for therapeutic and diagnostic radiometals in radiopharmaceutical elaboration.



INTRODUCTION

Over the last 20 years, radiopharmaceutical therapy (RPT) has emerged as an alternative for the treatment and diagnosis of cancer. Unlike traditional radiotherapy, where radiation beams are administered *ex vivo*, RPT involves delivering radiation payloads directly and specifically to cancer cells *in vivo*.¹ This method has several advantages over existing therapeutic strategies, including attenuated radiation dose, reduced side effects, and rapid drug response, and enables *in vivo* visualization through positron emission tomography (PET) or single-photon emission computed tomography (SPECT).¹

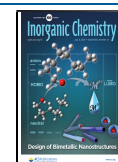
Metallic radioisotopes (also termed radiometals) possess vast diversity in terms of their physical properties (e.g., radiological half-life and decay emissions), making them ideal for incorporation into radiopharmaceuticals. A metal-based radiopharmaceutical can generally be broken down into four components consisting of the radiometal, bifunctional chelator (BFC), linker, and biomolecule/targeting vector.² The decay properties of the radiometal provide the diagnosis/treatment, while the biomolecule/targeting vector ensures accumulation of the drug at the point of infection. These two components are then combined through the BFC and linker. Several radiopharmaceuticals bearing this blueprint are currently in clinical trials,¹ and recently their potential was recognized with the FDA approval of lutetium-177 (^{177}Lu) Lu-DOTATATE, a radioactive drug used for the treatment of neuroendocrine tumors.³ BFCs contain a multidentate ligand, which coordinates the radionuclide, and a reactive arm that can be

covalently bound to the linker or targeting vector. Designing BFCs is a key component for a fully functioning inorganic radiopharmaceutical and must meet specific requirements to be optimal. These include being synthetically accessible, being able to bind the radiometal under radiopharmaceutical conditions (mild temperatures, submicromolar ligand concentrations, fast reaction times), and forming kinetically inert complexes which are stable to transchelation *in vivo*. This is an active area of research with several BFCs being developed over the years.^{4,5} For example, Figure 1 illustrates a handful of popular BFCs (1–4) used in nuclear medicine with different bifunctional arms and coordinating environments. There is, however, an opportunity for developing new ligands, and their bifunctional variants, for radiopharmaceutical purposes with the potential to surpass, in terms of function and application, those that are currently used.

[2.2.2]-cryptand (Kryptofix 222) 5 is a three-dimensional N_2O_6 donating “cage like” structure synthesized by Lehn in the late 1960s.^{6,7} Since its discovery, the ligand has demonstrated a myriad of applications in chromatography,^{8,9} organic syn-

Received: May 4, 2021

Published: June 23, 2021



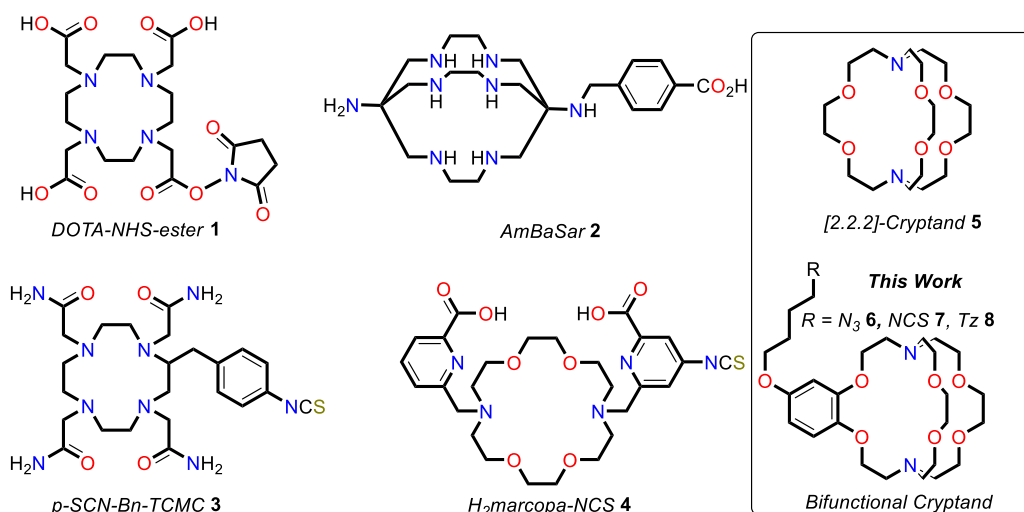


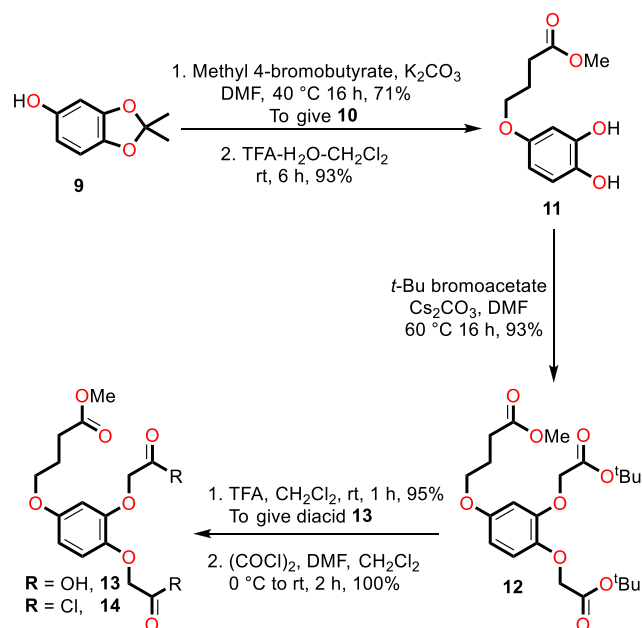
Figure 1. (left) Structures of popular bifunctional chelators. (right) Illustrating the concept for bifunctional [2.2.2]-cryptands developed in this work in comparison to the original structure.

thesis,¹⁰ crystallography,^{11–13} electrochemistry,^{14,15} chemical sensing,¹⁶ and magnetic resonance imaging.^{17–19} Surprisingly, to the best of our knowledge, [2.2.2]-cryptand has never been radiolabeled and developed into a BFC. Its only application in radiochemistry is as a phase-transfer catalyst when synthesizing the PET imaging agent [¹⁸F]fluoro-2-deoxy-2-D-glucose ([¹⁸F]-FDG).²⁰ Some N₆ donating cryptands, such as DiAmSar and its subsequent bifunctional analogues (e.g., AmBaSar 2, Figure 1), have been developed for copper-64 and -67 (⁶⁴Cu/⁶⁷Cu) radiolabeling and form remarkably kinetically inert Cu complexes.^{21–24} However, synthesizing the bifunctional analogues can be challenging, and its small cavity size limits its application to only small radionuclides. It is therefore worth investigating if the [2.2.2]-cryptand could be made bifunctional and radiolabeled for nuclear medicine applications. The pioneering work for [2.2.2]-cryptand-metal complexes has primarily focused on alkali metal cations. However, very recently the ligand has been demonstrated to coordinate lanthanides, actinides, and other large metal cations analogous to radiometals. These complexes exhibit extraordinary thermodynamic and kinetic stability and are highly resistant toward transchelation.^{12,25–28} We rationalized that the trend may carry over to radiometals and potentially lead to new ligands that bind radiometals under radiopharmaceutical conditions (*vide supra*) to form exceptionally thermodynamically stable and kinetically inert complexes *in vivo*. The main challenge would be making the cryptand bifunctional and employing a reproducible synthetic route that could be easily implemented. The original structure was therefore redesigned to contain an aromatic functionality bearing a novel bifunctional arm (Figure 1, structures 6–8). Disclosed herein are the results of this investigation which illustrate the first synthesis of three bifunctional [2.2.2]-cryptands for potential use in imaging, targeted or pretargeted RPT. Their bifunctional utility was demonstrated, and proof of principle radiolabeling was undertaken and optimized with γ -emitter lead-203 (²⁰³Pb, *t*_{1/2} = 51.9 h). Finally, the first CRYPT-radioimmunoconjugates was synthesized by coupling to the HER2/*neu*-targeting monoclonal antibody (mAb) trastuzumab (Herceptin).^{29–31}

RESULTS AND DISCUSSION

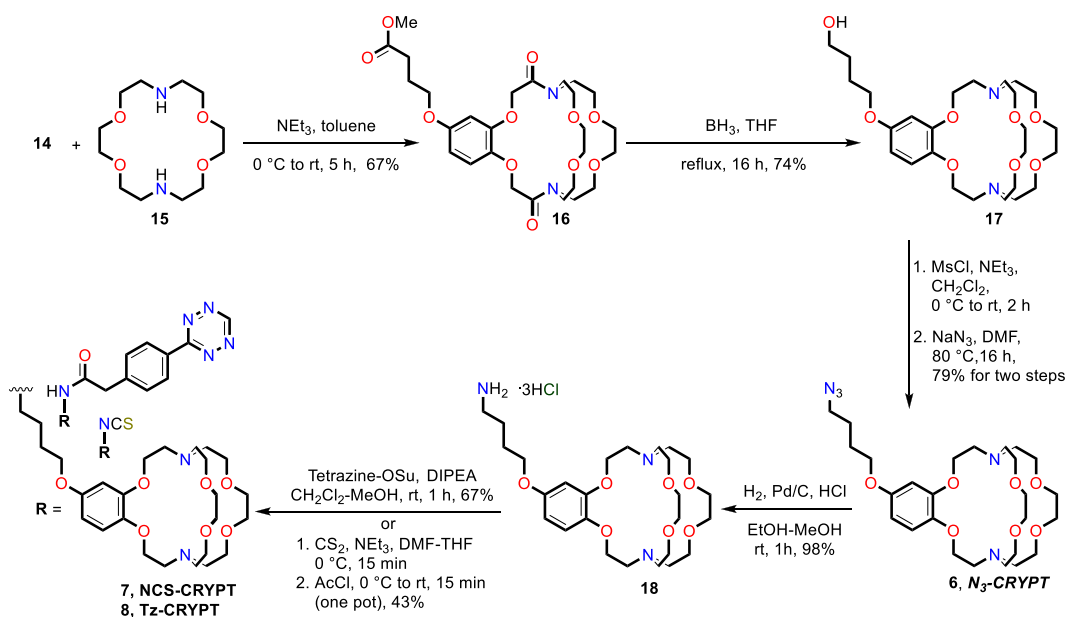
Synthesis and Characterization. The synthesis began by transforming phenol³² **9** into the required bifunctional arm **14** (Scheme 1). Alkylation of **9** with methyl 4-bromobutyrate gave

Scheme 1. Synthesis of Bifunctional Arm 14



intermediate **10**, which was subsequently treated with aqueous trifluoroacetic acid (TFA) to give **11** in excellent yield (66% for two steps). The alkylation deprotection protocol was then repeated by treating **11** with *tert*-butyl bromoacetate under basic conditions to give **12**; the *tert*-butyl esters were then removed with TFA to give diacid **13**. Treating **13** with oxalyl chloride then gave **14** in quantitative yield (88% for three steps). With the diacid chloride intermediate **14** in hand, amide coupling to 4,13-diaza-18-crown-6 **15** was undertaken (Scheme 2). High dilution in toluene for this transformation is necessary to obtain diamide **16** in good yield (67%).¹⁹ Following this, chemoselective reduction of the amide over the

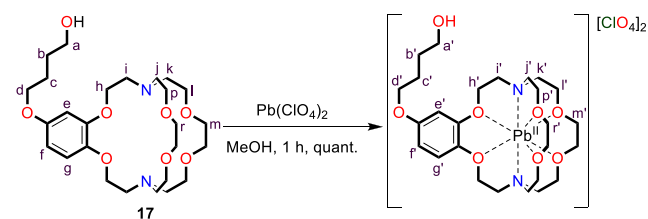
Scheme 2. Synthesis of the Bifunctional [2.2.2]-Cryptands 6, 7, and 8



ester in **16** was attempted with 9-BBN.³³ The initial synthetic design for a bifunctional cryptand was to perform a chemoselective reduction of the amide, saponify the ester to the corresponding acid, and then convert into a succinimidyl ester. However, the transformation with 9-BBN was unsuccessful, giving poor yield of the desired product and complex reaction mixtures. **16** was therefore treated with borane-tetrahydrofuran (BH₃-THF) to simultaneously reduce the diamide and the methyl ester to give cryptand **17** in good yield (74%).¹⁹ Oxidation of the primary alcohol on **17** to the corresponding carboxylic acid was unsuccessful with TEMPO/BAIB,³⁴ Jones Reagent,³⁵ and with pyridinium dichromate in DMF.³⁶

Activation of the alcohol with triphosgene and disuccinimidyl carbonate (DSC) was also attempted. Both the chloroformate and succinimidyl carbamate could be detected and trapped with a primary amine to give the corresponding carbamate. However, purification of the products was too difficult and not reproducible. It was therefore decided to convert the alcohol to an azide by treating **17** with methane sulfonyl chloride to give the corresponding mesylate, which was immediately treated with sodium azide (NaN₃) in DMF at 80 °C to give **6** in excellent yield (79% for two steps).³⁷ It is worth noting that the azide-cryptand (N₃-CRYPT) **6** is bifunctional and can be used for strained promoted azide-alkyne cycloaddition (SPAAC) to synthesize bioconjugates.³⁸ Following this, **6** was transformed to primary amine **18** via palladium-catalyzed hydrogenation in almost quantitative yield (98%). To complete the synthesis, the amino-cryptand was then converted into two more novel bifunctional cryptands. **18** was treated with carbon disulfide, to give an intermediate dithiocarbamate, which was transformed *in situ* with acetyl chloride to the corresponding isothiocyanate-cryptand (NCS-CRYPT) **7** in moderate yield (43%). Alternatively, **18** can be conjugated with tetrazine-NHS ester³⁹ to give tetrazine-cryptand (Tz-CRYPT) **8** in good yield (67%). In general, starting from the diacid chloride intermediate **14**, each of the bifunctional cryptands **6**, **7**, or **8** can be prepared in under 5 days.

Our attention then turned to choosing a suitable radiometal for the cryptand. Of the number of radioisotopes available, and with the cavity size of [2.2.2]-cryptand being 2.8 Å, we hypothesized that the diagnostic radiometal ²⁰³Pb^{II} (*t*_{1/2} = 52 h, ionic radius = 1.29 Å for coordination number (CN) = 8)⁴⁰ would fit within the cryptand cavity; ²⁰³Pb is also readily available via irradiation of thallium on a medical cyclotron and produced regularly at our facility. Moreover, the cryptand provides potentially 8-donor atoms of borderline to moderate basicity, two 3° amines and six ether oxygens, which we believed would satisfy the coordination chemistry of Pb(II) which is characterized as a borderline Lewis acid according to Pearson's hard soft acid base theory. Prior to radiolabeling studies, the nonradioactive ^{nat}Pb^{II}-cryptand complex was prepared and characterized. Gratifyingly, upon treating **17** with lead(II) perchlorate (Pb(ClO₄)₂), the corresponding cryptand lead complex [Pb(**17**)ClO₄][ClO₄] was isolated in quantitative yield (Scheme 3). The ¹H NMR spectrum of

Scheme 3. Synthesis of Nonradioactive Lead(II) Complex [Pb(**17**)ClO₄][ClO₄] from Pb(ClO₄)₂ with ¹H NMR Labeling Assignments

[Pb(**17**)ClO₄][ClO₄] (Figure 2) showed clear downfield shifts for each CH₂ within the cryptand core compared to the uncoordinated ligand **17**, thereby suggesting that each heteroatom was interacting to form an 8-coordinate solution structure. There was no dramatic chemical shift change with the side arm methylene protons, indicating that this moiety played no part in forming the complex. The ¹H NMR also confirms that only one highly symmetric isomer is present in

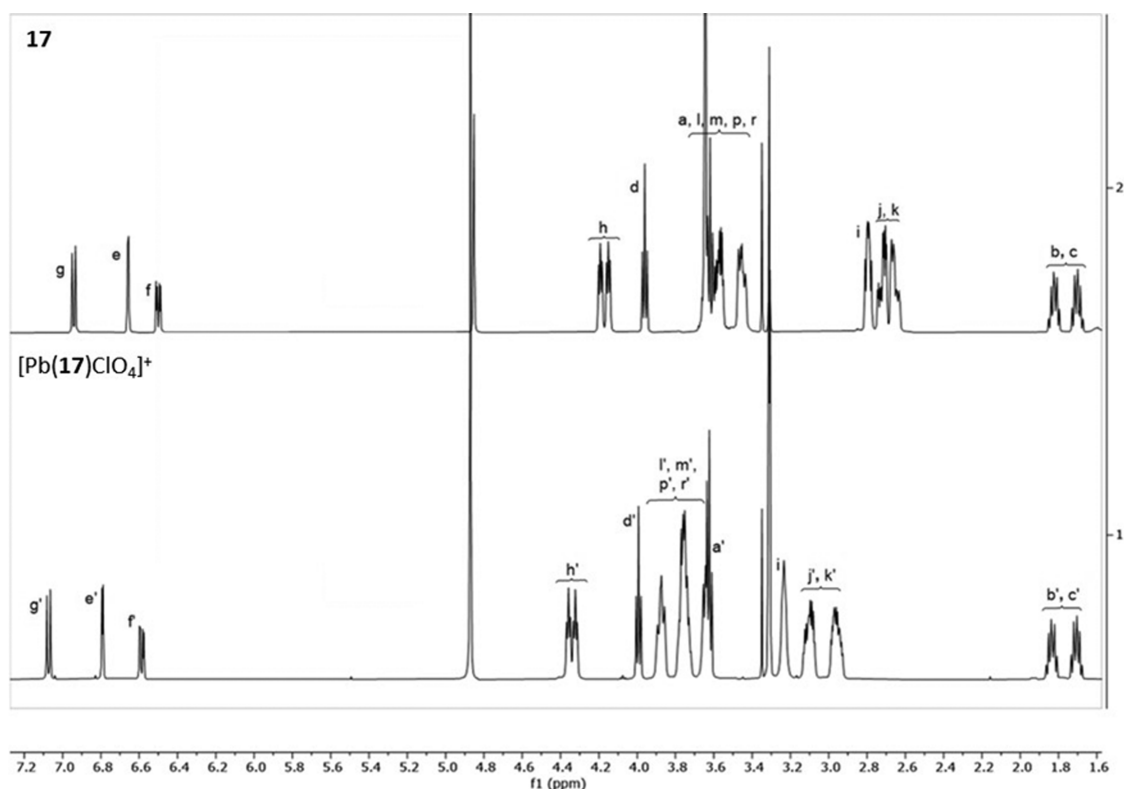


Figure 2. ^1H NMR (500 MHz) spectra in $\text{CD}_3\text{OD}-d_4$ at ambient temperature of ligand **17** (top) and the corresponding lead complex $[\text{Pb}(\text{17})\text{ClO}_4]^+$ (bottom).

solution, an advantage because complexes that form a minimum number of isomers are more stable *in vivo*, which is a key component for a successful radiopharmaceutical.^{41,42}

Next was to gain insight into the solid-state structure; however, crystallization attempts of $[\text{Pb}(\text{17})\text{ClO}_4][\text{ClO}_4]$ were unsuccessful. It was rationalized the side arm might be influencing crystal growth. Instead, the core [2.2.2]-cryptand structure bearing no functional side arm (**19**) was synthesized via a novel route similar to **17** (see the Supporting Information) and reacted with $\text{Pb}(\text{ClO}_4)_2$ to give $[\text{Pb}(\text{19})\text{ClO}_4][\text{ClO}_4]$ from which X-ray quality crystals were obtained through vapor diffusion (Figure 3). The X-ray structure shows Pb^{II} residing in the center of the cryptand bound by the eight N_2O_6 donor atoms (suggested by ^1H NMR) as well as one perchlorate counterion through both O atoms to form a 10-coordinate complex. The bond lengths for $[\text{Pb}(\text{19})\text{ClO}_4]$ -

$[\text{ClO}_4]$ (N–Pb (2.8 Å), aliphatic O–Pb (~ 2.6 Å), aromatic O–Pb (2.9, 3.0 Å), and perchlorate O–Pb (2.9 Å)) are similar to $[\text{U}(\text{crypt})\text{I}_2][\text{I}]$,²⁵ $[\text{Nd}(\text{crypt})\text{OTf}_2][\text{OTf}]$,²⁷ and $[\text{Eu}(\text{crypt})\text{Cl}][\text{Cl}]$ ¹⁹ metal complexes. The ionic radius for Pb^{II} (1.4 Å for coordination number (CN) = 10) is slightly larger than but comparable to that for Eu^{2+} , La^{3+} , U^{3+} , and Nd^{3+} when coordinated to cryptands (Table 1).

Prior to radiolabeling studies, the bifunctional application of cryptands NCS-CRYPT (**7**) and Tz-CRYPT (**8**) was demonstrated. The isothiocyanate (–NSC) and tetrazine (–Tz) functionalities can be employed in targeted or pretargeted radiopharmaceutical formulation, respectively.

Table 1. Comparing the Bond Lengths of $[\text{Pb}(\text{19})\text{ClO}_4][\text{ClO}_4]$ and Metal Atomic Radii with Literature Metal–[2.2.2]-Cryptand Complexes^a

M–crypt complex	bond length (Å)			
	N–M	O–M aliphatic	O–M aromatic	M–Ionic radius (CN) ^b
$[\text{Pb}(\text{19})\text{ClO}_4][\text{ClO}_4]$	2.8	2.6	2.9, 3.0	1.4 (10)
$[\text{Eu}(\text{crypt})\text{Cl}][\text{Cl}]$ ¹⁹	2.8	2.7	2.7, 2.8	1.3 (9)
$[\text{La}(\text{crypt})\text{Cl}_2][\text{Cl}]$ ²⁵	2.9	2.7	NA	1.27 (10)
$[\text{U}(\text{crypt})\text{I}_2][\text{I}]$ ²⁵	2.8, 2.9	2.57, 2.70	NA	ND ^c (10)
$[\text{Nd}(\text{crypt})\text{OTf}_2][\text{OTf}]$ ²⁷	2.8	2.55, 2.6	NA	ND ^d (10)

^aNA (not applicable) refers to structures that do not contain an aromatic ring O–M bond length. CN, coordination number. ^bReported metal ionic radii taken from.⁴⁰ ^cND = not determined (no reported value for U(III) ion [CN = 10]; ionic radius for U(III) ion [CN = 6] reported as 1.03 Å). ^dND = not determined (no reported value for Nd(III) ion [CN = 10]; ionic radii for Nd(III) [CN = 9, 12] reported as 1.16 and 1.27 Å, respectively).

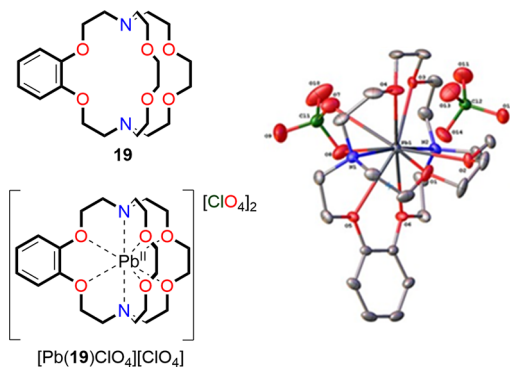
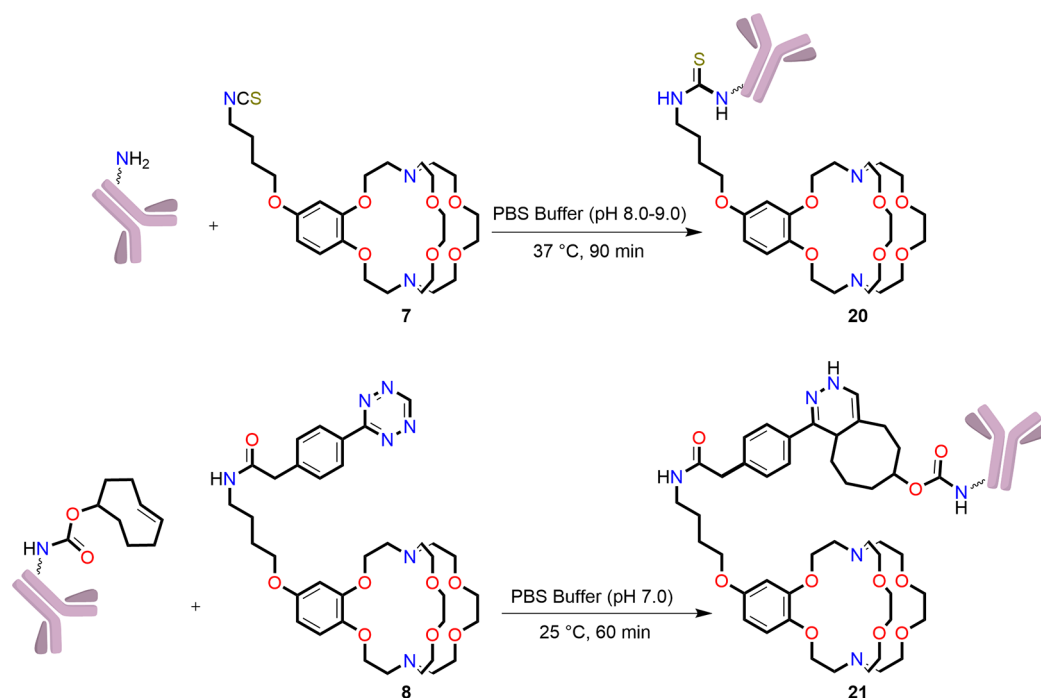


Figure 3. Solid-state X-ray crystal structure of $[\text{Pb}(\text{19})\text{ClO}_4][\text{ClO}_4]$ synthesized from the core nonbifunctional cryptand **19**.

Scheme 4. Illustrating the Synthesis of Trastuzumab-Cryptand Immunoconjugates **20** and **21**, from NCS-CRYPT (**7**) and Trastuzumab (top) or from TCO-Trastuzumab and Tz-CRYPT (**8**) (bottom)^a



^aThe average number of ligands per antibody was determined by MALDI-TOF MS/MS to be 2.1 for **20** and 4.3 for **21**.

Generally, in targeted imaging or therapy, an immunoconjugate is synthesized from reacting the antibody lysine residues with the bifunctional arm (isothiocyanate, succinimide, azide, etc.) of a BFC, then labeled with a multiday half-life radionuclide, and injected *in vivo* to accumulate at a tumor. In pretargeted therapy, a *trans*-cyclooctene (TCO) modified antibody, which can only react with a tetrazine residue via the inverse electron-demand Diels–Alder (IEDDA) reaction, is administered *in vivo*. The antibody slowly accumulates at the tumor and clears from the blood. A radiolabeled chelator bearing a tetrazine is then injected and rapidly conjugates to only the TCO-antibody *in vivo*.^{43,44} Pretargeted therapy is becoming popular over targeted therapy because short-lived radionuclides can be utilized and the overall radiation dose is significantly reduced. The synthesized bifunctional cryptands therefore have potential to be used for targeted (N₃-CRYPT, NCS-CRYPT, and Tz-CRYPT) or pretargeted (Tz-CRYPT) therapy. As a proof of principle, the conjugation of the bifunctional cryptands **7** and **8** with the monoclonal antibody trastuzumab was investigated (Scheme 4). For the NCS-CRYPT (**7**), the conditions involved incubating the ligand with the antibody in PBS buffer (pH 8.0–9.0) at 37 °C for 90 min.⁴⁵ The conjugation with the Tz-CRYPT (**8**) was preformed with TCO-trastuzumab (synthesized as per previously published procedures)⁴⁴ and incubated in PBS buffer (pH 7.0) at 25 °C for 60 min.⁴⁶ After purifying each conjugation reaction via PD-10 size exclusion, both the corresponding thiourea **20** and 1,2-dihydropyrazine **21** immunoconjugates were confirmed by MALDI-TOF MS/MS. The average number of chelators per antibody were 2.1 for **20** and 4.3 for **21**.

Radiolabeling Experiments. With our novel bifunctional [2.2.2]-cryptands and immunoconjugates in hand, radiolabeling with [²⁰³Pb]Pb²⁺ was investigated. Because this

represents the first example of radiolabeling [2.2.2]-cryptands, it was predicted optimization would be necessary to obtain sufficient radiochemical yields (RCYs). OH-CRYPT (**17**) was therefore chosen as a model substrate to investigate the initial radiolabeling performance. Cryptands are reported to bind alkali metal (Li⁺, Na⁺, K⁺)^{47–49} and ammonium (NH₄⁺)⁵⁰ cations, and therefore, because radiolabeling reactions are generally carried out in buffers containing these cations, they may compete with the radiometal, especially at lower concentrations. Keeping this in mind, **17** ([L] = 10^{−4} M) was incubated with ²⁰³Pb (40–60 kBq)⁵² in either 1 or 0.1 M ammonium acetate (NH₄OAc, pH 7). Further, recent reports of improved radiolabeling yields in organic solvents compared to aqueous buffers motivated our investigation of ²⁰³Pb labeling in methanol (MeOH), ethanol (EtOH), acetonitrile (CH₃CN), and dimethyl sulfoxide (DMSO).⁵¹ Nonisolated RCYs were determined via radio-instant thin layer chromatography (radio-iTLC) after 5 and 60 min at room temperature or 80 °C. Complexation was observed at ambient temperature for each reaction with RCYs after 60 min of >99% (1 M NH₄OAc, pH 7), >99% (0.1 M NH₄OAc, pH 7), 94.2 ± 3.8% (MeOH), 94.6 ± 0.9% (EtOH), 94.7 ± 1.1% (CH₃CN), and 30.2 ± 2.4% (DMSO); *n* = 3 for each experiment. The reactions were incomplete after 5 min, and elevated temperature (80 °C) had no effect on rate or RCY. Because preliminary ²⁰³Pb labeling in organic solvents did not yield quantitative labeling, further experiments in MeOH, EtOH, CH₃CN or DMSO were not attempted. Concentration-dependent (10^{−4}–10^{−7} M) radiolabeling in 1 and 0.1 M NH₄OAc (pH 7) was conducted. The RCY in 1 M NH₄OAc unfortunately decreased significantly at 10^{−5} M (25.7 ± 4.6%; *n* = 3) and 10^{−6} M (3.8 ± 1.3%; *n* = 3) ligand concentration. However, the RCY with 0.1 M NH₄OAc at 10^{−5} M was >99%, *n* = 3 and 88.6% ± 6.0%, *n* = 3 for 10^{−6} M and suggests the NH₄⁺ was competing with ²⁰³Pb at higher

buffer concentrations. Using the optimized labeling conditions (0.1 M NH_4OAc , pH 7, room temperature, 60 min), a comparative labeling investigation between CRYPT 17 and commercial standards for ^{203}Pb chelation, DOTA, and TCMC (Figure 4), ($[\text{L}] = 10^{-4}$ – 10^{-7} M) was conducted. All three

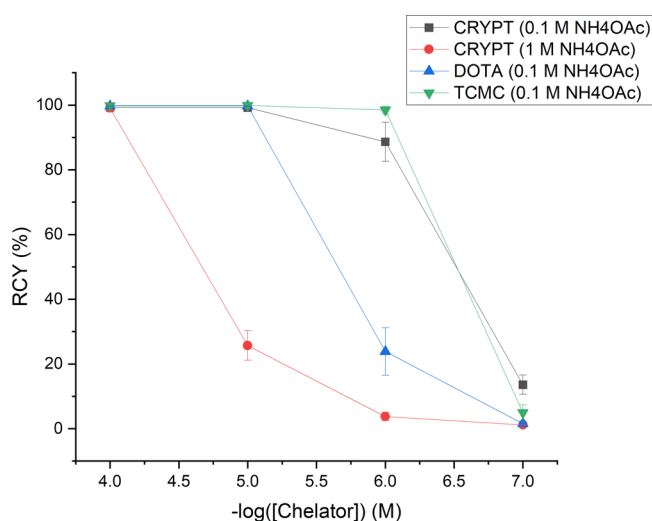


Figure 4. Radiochemical yields (RCYs) at various ligand concentrations for OH-CRYPT 17 (1 and 0.1 M NH_4OAc , pH 7), TCMC (0.1 M NH_4OAc , pH 7), and DOTA (0.1 M NH_4OAc , pH 7) complexation with $^{203}\text{Pb}(\text{OAc})_2$ at 1 h and room temperature.

ligands quantitatively (RCY > 99%) complexed ^{203}Pb at ligand concentrations of 10^{-4} and 10^{-5} M. At 10^{-6} M the RCY for DOTA dropped to $23.9 \pm 7.3\%$, $n = 3$ while TCMC maintained near quantitative RCYs ($98.4 \pm 1.2\%$, $n = 3$), and the CRYPT dropped to $88.6 \pm 6.0\%$, $n = 3$. Then at 10^{-7} M TCMC and DOTA were $5.0 \pm 2.4\%$ and $1.5 \pm 0.6\%$, respectively (each $n = 3$), and CRYPT was slightly higher at $13.6 \pm 3.0\%$, $n = 3$. These results suggest that, under these conditions, the cryptand is superior to DOTA and comparable to TCMC at complexing ^{203}Pb . The kinetic inertness of the resulting ^{203}Pb -CRYPT complex was evaluated in an *in vitro* human serum stability assay (Table 2). Radiopharmaceuti-

Table 2. Human Serum Stability Challenge Data Performed at 37 °C ($n = 3$), with Stability Shown as Percentage of Intact ^{203}Pb Complex

no. ^a	1–8 h	24 h	48 h	72 h
1	93.0 ± 1.0% (3 h)	92.0 ± 1.5%	94.0 ± 1.0%	91.6 ± 0.6%
2	97.2 ± 1.2% (1 h)	99.2 ± 1.1%	97.5 ± 1.3%	95.7 ± 0.6%
3	97.1 ± 0.7% (8 h)	97.3 ± 0.6%	98.1 ± 0.2%	97.4 ± 0.5%
4	98.0 ± 0.5% (8 h)	98.1 ± 0.2%	98.2 ± 0.3%	97.2 ± 0.7%

^a1 ^{203}Pb -OH-CRYPT, 2 ^{203}Pb -Tz-CRYPT, 3 ^{203}Pb -Pb-DOTA,⁵² and 4 ^{203}Pb -Pb-TCMC.⁵²

tics for targeted or pretargeted therapy are given by intravenous (IV) injection, and because several endogenous ligands, such as albumin and metallothionein, present in blood serum can compete and displace chelator bound metal ions, it is necessary to investigate if radiometal-chelate complexes can withstand transchelation *in vivo*. Failure to do so would result in unsuccessful delivery of the radiopharmaceuticals to the desired target. ^{203}Pb -CRYPT was incubated with human serum under physiological conditions (37 °C, pH 7), and the

percentage of intact ^{203}Pb was monitored by iTLC at 3 h, 24 h, 48 and 72 h. The complex remained >91% over the course of the study, thereby demonstrating exceptional stability for the radiolabeled cryptand.

Finally, to demonstrate the ability of the bifunctional cryptands to form radioimmunoconjugates, the optimized ^{203}Pb radiolabeling was performed with immunoconjugate 20 and Tz-CRYPT 8. As mentioned, targeted therapy involves a radiolabeled immunoconjugate, whereas in pretargeting, a tetrazine-bearing BFC is labeled and conjugated to a TCO-modified antibody. 20 (50, 25, or 10 μg) was incubated with ^{203}Pb (50 kBq) for 60 min at room temperature, and the corresponding radioimmunoconjugate formation was confirmed via iTLC for each reaction with RCYs of $88.1 \pm 0.1\%$, $83.2 \pm 0.4\%$, and $77.7 \pm 0.6\%$ ($n = 3$ for each experiment), respectively. Further, Tz-CRYPT 8 was radiolabeled with ^{203}Pb (50 kBq) in quantitative yield. The ^{203}Pb -Tz-CRYPT was observed to be stable in human serum over 72 h (Table 2), and the IEDDA reaction was performed by incubating the radioligand with TCO-trastuzumab at different molar ratios (2:1, 4:1, and 10:1 Tz-CRYPT to TCO-trastuzumab).⁴⁶ After 60 min at room temperature each reaction was purified via PD-10 size exclusion, and the corresponding radioimmunoconjugate was confirmed by γ spectroscopy of the final eluate to give radiolabeling yields of 51%, 60%, and 39%, respectively.

CONCLUSION

In summary, we have disclosed the synthesis of novel bifunctional [2.2.2]-cryptands and demonstrated their potential use in nuclear medicine for the first time. A novel bifunctional arm was synthesized in five steps with a 58% overall yield and conjugated to 4,13-diaza-18-crown-6. The corresponding diamide intermediate was conveniently transformed into three novel bifunctional cryptands bearing an azide (N_3 -CRYPT), an isothiocyanate (NCS-CRYPT), or a tetrazine (Tz-CRYPT) with 39%, 17%, and 26% overall yields, respectively. Nonradioactive Pb-complexes of OH-CRYPT (17) and the nonbifunctional analogue (CRYPT) were prepared and characterized; ^1H NMR suggested an 8-coordinate solution structure, which forms a single isomer. X-ray crystallography revealed a 10-coordinate solid-state structure bound by the eight N_2O_6 donor atoms as well as one perchlorate counterion. Furthermore, the bifunctional application for NCS-CRYPT and Tz-CRYPT was demonstrated by conjugating each BFC to the monoclonal antibody trastuzumab. CRYPT-radiolabeling was successful with SPECT imaging isotope ^{203}Pb ; the transformation then was optimized to obtain high RCYs. Finally, the preclinical application was demonstrated by synthesizing ^{203}Pb -CRYPT radioimmunoconjugates for targeted or pretargeted therapy. The success of this investigation highlights a potential application for CRYPT ligands in nuclear medicine. Herein, we have shown radiolabeling with $^{203}\text{Pb}^{2+}$; however, there are a myriad of radioisotopes available for testing ($^{225}\text{Ac}^{3+}$, $^{111}\text{In}^{3+}$, $^{64}\text{Cu}^{2+}$, $^{212}\text{Pb}^{2+}$, etc.). CRYPT could find use for many radiometals and lead to new radiopharmaceuticals to treat and diagnose diseases. Further experimentation is now underway and will be reported in due course.

■ ASSOCIATED CONTENT

Supporting Information

The Supporting Information is available free of charge at <https://pubs.acs.org/doi/10.1021/acs.inorgchem.1c01274>.

Experimental procedures, ^1H and ^{13}C NMR spectra, X-ray crystallography data, and iTLC and radio HPLC chromatograms (PDF)

Accession Codes

CCDC 2080228 contains the supplementary crystallographic data for this paper. These data can be obtained free of charge via www.ccdc.cam.ac.uk/data_request/cif, or by emailing data_request@ccdc.cam.ac.uk, or by contacting The Cambridge Crystallographic Data Centre, 12 Union Road, Cambridge CB2 1EZ, UK; fax: +44 1223 336033.

■ AUTHOR INFORMATION

Corresponding Author

Caterina F. Ramogida – Department of Chemistry, Simon Fraser University, Burnaby, BC V5A 1S6, Canada; Life Sciences Division, TRIUMF, Vancouver, BC V6T 2A3, Canada; orcid.org/0000-0003-4815-2647; Email: cfr@sfu.ca

Authors

Anthony W. McDonagh – Department of Chemistry, Simon Fraser University, Burnaby, BC V5A 1S6, Canada

Brooke L. McNeil – Department of Chemistry, Simon Fraser University, Burnaby, BC V5A 1S6, Canada; Life Sciences Division, TRIUMF, Vancouver, BC V6T 2A3, Canada

Brian O. Patrick – Department of Chemistry, University of British Columbia, Vancouver, BC V6T 1Z1, Canada; orcid.org/0000-0002-2921-8439

Complete contact information is available at:

<https://pubs.acs.org/doi/10.1021/acs.inorgchem.1c01274>

Notes

The authors declare no competing financial interest.

■ ACKNOWLEDGMENTS

Funding for this work was provided by Natural Sciences and Engineering Research Council (NSERC) of Canada Discovery Grant (CFR, RGPIN-2019-07207) and a Social Sciences and Humanities Research Council (SSHRC) of Canada New Frontiers in Research Fund Exploration Grant (CFR, NFRFE-2018-00499). TRIUMF receives funding via a contribution agreement with the Natural Research Council of Canada. The BC Cancer Agency (Dr. Julie Rousseau) is thanked for contributing trastuzumab for this study.

■ REFERENCES

- (1) Sgouros, G.; Bodei, L.; McDevitt, M. R.; Nedrow, J. R. Radiopharmaceutical Therapy in Cancer: Clinical Advances and Challenges. *Nat. Rev. Drug Discovery* **2020**, *19* (9), 589–608.
- (2) Kostelnik, T. I.; Orvig, C. Radioactive Main Group and Rare Earth Metals for Imaging and Therapy. *Chem. Rev.* **2019**, *119* (2), 902–956.
- (3) Strosberg, J.; Wolin, E.; Chasen, B.; Kulke, M.; Bushnell, D.; Caplin, M.; Baum, R. P.; Kunz, P.; Hobday, T.; Hendifar, A.; Oberg, K.; Sierra, M. L.; Thevenet, T.; Margalet, I.; Ruzsiewicz, P.; Krenning, E. Health-Related Quality of Life in Patients With Progressive Midgut Neuroendocrine Tumors Treated With (177)Lu-Dotatate in the Phase III NETTER-1 Trial. *J. Clin. Oncol.* **2018**, *36* (25), 2578–2584.

- (4) Thiele, N. A.; Brown, V.; Kelly, J. M.; Amor-Coarasa, A.; Jermilova, U.; MacMillan, S. N.; Nikolopoulou, A.; Ponnala, S.; Ramogida, C. F.; Robertson, A. K. H.; Rodríguez-Rodríguez, C.; Schaffer, P.; Williams, C.; Babich, J. W.; Radchenko, V.; Wilson, J. J. An Eighteen-Membered Macrocyclic Ligand for Actinium-225 Targeted Alpha Therapy. *Angew. Chem., Int. Ed.* **2017**, *56* (46), 14712–14717.

- (5) Chappell, L. L.; Dadachova, E.; Milenic, D. E.; Garmestani, K.; Wu, C.; Brechbiel, M. W. Synthesis, Characterization, and Evaluation of a Novel Bifunctional Chelating Agent for the Lead Isotopes 203Pb and 212Pb. *Nucl. Med. Biol.* **2000**, *27* (1), 93–100.

- (6) Dietrich, B.; Lehn, J. M.; Sauvage, J. P. Les Cryptates. *Tetrahedron Lett.* **1969**, *10* (34), 2889–2892.

- (7) Dietrich, B.; Lehn, J. M.; Sauvage, J. P. Diaza-Polyoxa-Macrocycles et Macrobicycles. *Tetrahedron Lett.* **1969**, *10* (34), 2885–2888.

- (8) Vanatta, L. E.; Woodruff, A.; Coleman, D. E. Comparison of Two Cryptand Separator Columns for the Determination of Trace Chloride in Semiconductor-Grade Nitric Acid. *J. Chromatogr. A* **2005**, *1085* (1), 33–36.

- (9) Woodruff, A.; Pohl, C. A.; Bordunov, A.; Avdalovic, N. Environmental Applications of a Cryptand Adjustable-Capacity Anion-Exchange Separator. *J. Chromatogr. A* **2003**, *997* (1–2), 33–39.

- (10) Landini, D.; Maia, A.; Montanari, F.; Tundo, P. Lipophilic [2.2.2] Cryptands as Phase-Transfer Catalysts. Activation and Nucleophilicity of Anions in Aqueous-Organic Two-Phase Systems and in Organic Solvents of Low Polarity. *J. Am. Chem. Soc.* **1979**, *101* (10), 2526–2530.

- (11) Chung, A. B.; Huh, D. N.; Ziller, J. W.; Evans, W. J. 2.2.2-Cryptand as a Bidentate Ligand in Rare-Earth Metal Chemistry. *Inorg. Chem. Front.* **2020**, *7* (22), 4445–4451.

- (12) Huh, D. N.; Ziller, J. W.; Evans, W. J. Facile Encapsulation of Ln(II) Ions into Cryptate Complexes from LnI 2 (THF) 2 Precursors (Ln = Sm, Eu, Yb). *Inorg. Chem.* **2019**, *58* (15), 9613–9617.

- (13) Goodwin, C. A. P.; Giansiracusa, M. J.; Greer, S. M.; Nicholas, H. M.; Evans, P.; Vonci, M.; Hill, S.; Chilton, N. F.; Mills, D. P. Isolation and Electronic Structures of Derivatized Manganocene, Ferrocene and Cobaltocene Anions. *Nat. Chem.* **2021**, *13*, 243.

- (14) Britz, D.; Knittel, D. Kryptate Complexes—Adsorption at Electrodes and Their Potential Electrochemical Use. *Electrochim. Acta* **1975**, *20* (11), 891–893.

- (15) Zejli, H.; Hidalgo-Hidalgo de Cisneros, J. L.; Naranjo-Rodriguez, I.; Elbouhouti, H.; Choukairi, M.; Bouchta, D.; Tamsamani, K. R. Electrochemical Analysis of Mercury Using a Kryptofix Carbon-Paste Electrode. *Anal. Lett.* **2007**, *40* (14), 2788–2798.

- (16) Li, J.; Yim, D.; Jang, W.-D.; Yoon, J. Recent Progress in the Design and Applications of Fluorescence Probes Containing Crown Ethers. *Chem. Soc. Rev.* **2017**, *46* (9), 2437–2458.

- (17) Garcia, J.; Neelavalli, J.; Haacke, E. M.; Allen, M. J. EuII-Containing Cryptates as Contrast Agents for Ultra-High Field Strength Magnetic Resonance Imaging. *Chem. Commun.* **2011**, *47* (48), 12858.

- (18) Garcia, J.; Allen, M. J. Interaction of Biphenyl-Functionalized Eu2+-Containing Cryptate with Albumin: Implications to Contrast Agents in Magnetic Resonance Imaging. *Inorg. Chim. Acta* **2012**, *393*, 324–327.

- (19) Ekanger, L. A.; Polin, L. A.; Shen, Y.; Haacke, E. M.; Martin, P. D.; Allen, M. J. A Eu II -Containing Cryptate as a Redox Sensor in Magnetic Resonance Imaging of Living Tissue. *Angew. Chem., Int. Ed.* **2015**, *54* (48), 14398–14401.

- (20) Jacobson, O.; Kiesewetter, D. O.; Chen, X. Fluorine-18 Radiochemistry, Labeling Strategies and Synthetic Routes. *Bioconjugate Chem.* **2015**, *26* (1), 1–18.

- (21) Di Bartolo, N. M.; Sargeson, A. M.; Donlevy, T. M.; Smith, S. V. Synthesis of a New Cage Ligand, SarAr, and Its Complexation with Selected Transition Metal Ions for Potential Use in Radioimaging†. *J. Chem. Soc. Dalton Trans.* **2001**, *15*, 2303–2309.

- (22) Liu, S.; Li, D.; Huang, C.-W.; Yap, L.-P.; Park, R.; Shan, H.; Li, Z.; Conti, P. S. The Efficient Synthesis and Biological Evaluation of Novel Bi-Functionalized Sarcophagine for ^{64}Cu Radiopharmaceuticals. *Theranostics* **2012**, *2* (6), 589–596.
- (23) Mume, E.; Asad, A.; Di Bartolo, N. M.; Kong, L.; Smith, C.; Sargeson, A. M.; Price, R.; Smith, S. V. Synthesis of Hexa Aza Cages, SarAr-NCS and AmBaSar and a Study of Their Metal Complexation, Conjugation to Nanomaterials and Proteins for Application in Radioimaging and Therapy. *Dalt. Trans.* **2013**, *42* (40), 14402.
- (24) Keinänen, O.; Fung, K.; Brennan, J. M.; Zia, N.; Harris, M.; van Dam, E.; Biggin, C.; Hedt, A.; Stoner, J.; Donnelly, P. S.; Lewis, J. S.; Zeglis, B. M. Harnessing ^{64}Cu / ^{67}Cu for a Theranostic Approach to Pretargeted Radioimmunotherapy. *Proc. Natl. Acad. Sci. U. S. A.* **2020**, *117* (45), 28316–28327.
- (25) Huh, D. N.; Windorff, C. J.; Ziller, J. W.; Evans, W. J. Synthesis of Uranium-in-Cryptand Complexes. *Chem. Commun.* **2018**, *54* (73), 10272–10275.
- (26) Gamage, N.-D. H.; Mei, Y.; Garcia, J.; Allen, M. J. Oxidatively Stable, Aqueous Europium(II) Complexes through Steric and Electronic Manipulation of Cryptand Coordination Chemistry. *Angew. Chem., Int. Ed.* **2010**, *49* (47), 8923–8925.
- (27) Huh, D. N.; Ciccone, S. R.; Bekoe, S.; Roy, S.; Ziller, J. W.; Furche, F.; Evans, W. J. Synthesis of Ln II -in-Cryptand Complexes by Chemical Reduction of Ln III -in-Cryptand Precursors: Isolation of a Nd II -in-Cryptand Complex. *Angew. Chem., Int. Ed.* **2020**, *59* (37), 16141–16146.
- (28) Swidan, A.; Macdonald, C. L. B. Polyether Complexes of Groups 13 and 14. *Chem. Soc. Rev.* **2016**, *45* (14), 3883–3915.
- (29) Woo, S.-K.; Jang, S. J.; Seo, M.-J.; Park, J. H.; Kim, B. S.; Kim, E. J.; Lee, Y. J.; Lee, T. S.; An, G. I.; Song, I. H.; Seo, Y.; Kim, K. I.; Kang, J. H. Development of ^{64}Cu -NOTA-Trastuzumab for HER2 Targeting: A Radiopharmaceutical with Improved Pharmacokinetics for Human Studies. *J. Nucl. Med.* **2019**, *60* (1), 26–33.
- (30) Massicano, A. V. F.; Marquez-Nostra, B. V.; Lapi, S. E. Targeting HER2 in Nuclear Medicine for Imaging and Therapy. *Mol. Imaging* **2018**, *17*, 153601211774538.
- (31) Li, L.; Rousseau, J.; Jaraquemada-Peláez, M. d. G.; Wang, X.; Robertson, A.; Radchenko, V.; Schaffer, P.; Lin, K.-S.; Bénard, F.; Orvig, C. ^{225}Ac -H₄py4pa for Targeted Alpha Therapy. *Bioconjugate Chem.* **2020**. DOI: 10.1021/acs.bioconjchem.0c00171
- (32) Fujiwara, K.; Sato, T.; Sano, Y.; Norikura, T.; Katoono, R.; Suzuki, T.; Matsue, H. Total Synthesis of Thelephantin O, Vialinin A/ Terrestriin A, and Terrestriins B–D. *J. Org. Chem.* **2012**, *77* (11), 5161–5166.
- (33) Flaniken, J. M.; Collins, C. J.; Lanz, M.; Singaram, B. Aminoborohydrides. 11. Facile Reduction of N -Alkyl Lactams to the Corresponding Amines Using Lithium Aminoborohydrides. *Org. Lett.* **1999**, *1* (5), 799–801.
- (34) van den Bos, L. J.; Codée, J. D. C.; van der Toorn, J. C.; Boltje, T. J.; van Boom, J. H.; Overkleeft, H. S.; van der Marel, G. A. Thioglycuronides: Synthesis and Application in the Assembly of Acidic Oligosaccharides. *Org. Lett.* **2004**, *6* (13), 2165–2168.
- (35) Bowden, K.; Heilbron, I. M.; Jones, E. R. H.; Weedon, B. C. L. 13. Researches on Acetylenic Compounds. Part I. The Preparation of Acetylenic Ketones by Oxidation of Acetylenic Carbinols and Glycols. *J. Chem. Soc.* **1946**, 39–45.
- (36) Corey, E. J.; Schmidt, G. Useful Procedures for the Oxidation of Alcohols Involving Pyridinium Dichromate in Aprotic Media. *Tetrahedron Lett.* **1979**, *20* (5), 399–402.
- (37) Pilgrim, W.; Murphy, P. V. α -Glycosphingolipids via Chelation-Induced Anomerization of O - and S -Glucuronic and Galacturonic Acid Derivatives. *Org. Lett.* **2009**, *11* (4), 939–942.
- (38) Pickens, C. J.; Johnson, S. N.; Pressnall, M. M.; Leon, M. A.; Berkland, C. J. Practical Considerations, Challenges, and Limitations of Bioconjugation via Azide–Alkyne Cycloaddition. *Bioconjugate Chem.* **2018**, *29* (3), 686–701.
- (39) Qu, Y.; Sauvage, F.-X.; Clavier, G.; Miomandre, F.; Audebert, P. Metal-Free Synthetic Approach to 3-Monosubstituted Unsymmetrical 1,2,4,5-Tetrazines Useful for Bioorthogonal Reactions. *Angew. Chem., Int. Ed.* **2018**, *57* (37), 12057–12061.
- (40) Shannon, R. D. Revised Effective Ionic Radii and Systematic Studies of Interatomic Distances in Halides and Chalcogenides. *Acta Crystallogr., Sect. A: Cryst. Phys., Diffraction, Theor. Gen. Crystallogr.* **1976**, *32* (5), 751–767.
- (41) Price, E. W.; Cawthray, J. F.; Bailey, G. A.; Ferreira, C. L.; Boros, E.; Adam, M. J.; Orvig, C. H₄octapa: An Acyclic Chelator for ^{111}In Radiopharmaceuticals. *J. Am. Chem. Soc.* **2012**, *134* (20), 8670–8683.
- (42) Liu, S.; Edwards, D. S. Bifunctional Chelators for Therapeutic Lanthanide Radiopharmaceuticals. *Bioconjugate Chem.* **2001**, *12* (1), 7–34.
- (43) Zeglis, B. M.; Sevak, K. K.; Reiner, T.; Mohindra, P.; Carlin, S. D.; Zanzonico, P.; Weissleder, R.; Lewis, J. S. A Pretargeted PET Imaging Strategy Based on Bioorthogonal Diels–Alder Click Chemistry. *J. Nucl. Med.* **2013**, *54* (8), 1389–1396.
- (44) Membreno, R.; Cook, B. E.; Zeglis, B. M. Pretargeted Radioimmunotherapy Based on the Inverse Electron Demand Diels–Alder Reaction. *J. Visualized Exp.* **2019**, e59041.
- (45) Zeglis, B. M.; Lewis, J. S. The Bioconjugation and Radiosynthesis of ^{89}Zr -DFO-Labeled Antibodies. *J. Visualized Exp.* **2015**, e52521.
- (46) Poty, S.; Membreno, R.; Glaser, J. M.; Ragupathi, A.; Scholz, W. W.; Zeglis, B. M.; Lewis, J. S. The Inverse Electron-Demand Diels–Alder Reaction as a New Methodology for the Synthesis of ^{225}Ac -Labelled Radioimmunoconjugates. *Chem. Commun.* **2018**, *54* (21), 2599–2602.
- (47) Šumanovac Ramljak, T.; Despotović, I.; Bertoša, B.; Mlinarić-Majerski, K. Synthesis and Alkali Metal Complexation Studies of Novel Cage-Functionalized Cryptands. *Tetrahedron* **2013**, *69* (49), 10610–10620.
- (48) Huh, D. N.; Darago, L. E.; Ziller, J. W.; Evans, W. J. Utility of Lithium in Rare-Earth Metal Reduction Reactions to Form Non-traditional Ln²⁺ Complexes and Unusual [Li(2.2.2-Cryptand)]¹⁺ Cations. *Inorg. Chem.* **2018**, *57* (4), 2096–2102.
- (49) Mamardashvili, G. M.; Maltceva, O. V.; Mamardashvili, N. Z.; Nguyen, N. T.; Dehaen, W. Cation Assisted Complexation of Octacarbazolyphenyl Substituted Zn(II)-Tetraphenylporphyrin with [2,2,2]Cryptand. *RSC Adv.* **2015**, *5* (55), 44557–44562.
- (50) Wang, X.; Shyshov, O.; Hanževački, M.; Jäger, C. M.; von Delius, M. Ammonium Complexes of Orthoester Cryptands Are Inherently Dynamic and Adaptive. *J. Am. Chem. Soc.* **2019**, *141* (22), 8868–8876.
- (51) Pérez-Malo, M.; Szabó, G.; Eppard, E.; Vagner, A.; Brücher, E.; Tóth, I.; Maiocchi, A.; Suh, E. H.; Kovács, Z.; Baranyai, Z.; Rösch, F. Improved Efficacy of Synthesizing $^{*}\text{M III}$ -Labeled DOTA Complexes in Binary Mixtures of Water and Organic Solvents. A Combined Radio- and Physicochemical Study. *Inorg. Chem.* **2018**, *57* (10), 6107–6117.
- (52) McNeil, B. L.; Robertson, A. K. H.; Fu, W.; Yang, H.; Hoehr, C.; Ramogida, C. F.; Schaffer, P. Production, Purification, and Radiolabeling of the $^{203}\text{Pb}/^{212}\text{Pb}$ Theranostic Pair. *EJNMMI Radiopharm. Chem.* **2021**, *6* (1), 6.